Archives Italiennes de Biologie, 145: 263-275, 2007.

THE LOCUST OLFACTORY SYSTEM AS A CASE STUDY FOR MODELING DYNAMICS OF NEUROBIOLOGICAL NETWORKS: FROM DISCRETE TIME NEURONS TO CONTINUOUS TIME NEURONS

B. QUENET [1] AND G. HORCHOLLE-BOSSAVIT [2]

[1] Equipe de Statistique Appliquée; [2] UMR CNRS 7084 ESPCI, 10 rue Vauquelin, 75005 PARIS

INTRODUCTION

For a long time, it was considered that neurons process or/and code information via firing rates. The precise timing of spikes was thought to be an irrelevant feature of a random Poisson process and most of experimental results were interpreted according to this point of view. As a consequence, theoretical models were built in terms of rate coding. Recent analysis at a fine time scale of *simultaneous neuronal activities* demonstrated the importance of precisely timed spike trains as well as *synchronization* in some neuron clusters. These data raised new issues about the use of both spatial and temporal information in coding processes, notably in sensory systems which deal with this general question: how the nervous system transforms afferent signals provided by sensory receptors into internal representations and code sensory information in the subsequent stages of the sensory pathways? Let us take the example of olfaction (6, 7, 9, 14), the set of sensory receptors which are activated by a specific odorant stimulus represents a *spatial mapping* of this stimulus. The complex *spatio-temporal patterns* built at the next stage of the olfactory system form the input to the level where discrimination, storage, and retrieval of stimuli are supposed to be performed (10).

The dynamical properties of the neuron assemblies are largely determined by their connectivity, i.e. the distribution of connections, by the strength of the synaptic contacts, by the propagation delays and by the input they receive. As soon as recurrent connectivity occurs between non-linear units, the relationship between the network architecture and the dynamical properties of the units are complex, and not yet fully understood. However, such dynamical properties play a major role in processing information and in learning, as they are the basis of coding. In addition they may participate to a "remodeling" of the architecture by inducing synaptic modifications. This is why the analysis of structure-function relationship is so important, even if complex.

In this context, the locust olfactory system can be considered as a case study for several reasons: 1) a relatively limited number of neurons and 2) a large corpus of biological data about synaptic connectivity, firing patterns, associative learning pro-

Corresponding Author: Dr: Brigitte Quenet. Tel: +33140794461. E-mail: brigitte.quenet@espci.fr

cedures (1, 2, 6, 7, 9, 10, 14). This system provides an appropriate framework for theoretical studies aiming at understanding how networks process spatial and temporal dimensions for coding information (1, 2). In short, an olfactory stimulus activates thousands of receptor neurons and induces temporally structured activities in some of the hundreds of the projection neurons (PN) and local interneurons (LN) at the level of the Antennal Lobe (AL). These activities result in an *oscillatory* local field potential (LFP): the oscillations persist after ablation of the neurons which are the PN targets, i.e the Kenyon cells in the Mushroom Body (6, 7, 10), which strongly suggests that these oscillations are driven by the PN themselves. In the coding process, it seems that each odor is discriminated not simply by an ensemble of synchronized neurons but mainly by a specific time evolution of their spiking. Some neurons are synchronized only during one or several epochs of the oscillatory response.

There are many models of the insect olfactory network, and simulations implementing integrate-and-fire or detailed conductance-based neuron models exhibit the type of complex dynamics experimentally observed in response to stimulus (1, 2). Detailed conductance-based neuron models with many ion channels of the Hodgkin-Huxley type require the definition of a large set of parameters featuring specific neuron properties. In addition, several functions are needed to describe the synaptic conductances involved in the connections between neurons. These models capture the fine modulations of membrane polarization and produce distributions of action potential timings which can be compared to those observed in experimental data. However, in these models, the effects of intrinsic properties of neurons and synapse types are indissociable from the network configuration: therefore, it is very difficult to analyze, for instance, what are the connectivity parameters responsible for resulting dynamics.

We have attempted to tackle this problem by constructing networks of simple time-discrete McCulloch and Pitts neurons (MC-P) (11). We previously demonstrated that small MC-P networks allow an analytical approach for computing appropriate synaptic matrix and input vectors compatible with specific binary spatio-temporal codes (4). In addition, we showed that using the same computed synaptic matrix, a network of Hodgkin-Huxley type neurons with an adapted time scale produces the same coding sequences. Here, we show that large MC-P networks are able to exhibit rich types of dynamics, from which *both oscillations and distributed synchrony may co-emerge*. Then we show that it is possible to use the designed connectivity matrix in MC-P networks in more realistic neuron models and to get similar dynamics, provided an appropriate "time grid". Thus MC-P networks, whose dynamics is entirely defined by the network configuration and the input, appears as the best tool in order to understand how the activity patterns are generated in recurrent networks. With such models, we approach a possible definition of the respective roles of the input, of the network connections and of the delays in driving the network towards chaotic behavior, oscillations or clusters of neurons firing synchronously.

METHODS

I - Time discrete McCulloch and Pitts neurons (MC-P)

A. The network model of MC-P units.

Our model is a fully connected network of MC-P units whose binary states are 0 or 1. The units are updated synchronously according to Eq. 1.

$$n_i(t) = H\left(\sum_{j=1}^{N} w_{ij} \cdot n_i\left(t - \tau_{ij}\right) + R_i - \frac{1}{2}\right) \qquad \text{Eq 1}$$

Here $n_i(t)$ is the binary state, 0 or 1, of neuron i at time t, W_{ij} is the synaptic weight from neuron j to neuron i, τ_{ij} is the transmission delay from neuron j to neuron i, R_i is an external input to neuron i, and H is the Heaviside function, whose value is nil if its argument is non positive, and 1 if its argument is strictly positive. The random connectivity of the network was set according to the following rules: in the connection matrix encoding the synaptic weights (if not nil, these weights are W_{ex} and W_{in} respectively for excitatory and inhibitory connections), every excitatory and inhibitory neuron sends an equal number of contacts, respectively to K_{ex} and K_{in} post-synaptic neurons, chosen at random. This leads to a recurrent synaptic architecture. In addition, a random set of neurons receives an input from K_r units representing the synaptic input from sensory receptors with a W_r weight. A *non-uniform matrix delay* takes into account different transmission delays: here τ_{ij}=1, i.e. one time step of the parallel update of the MC-P units, when neuron j is excitatory and τ_{ij}=2, when it is inhibitory.

B. *A descriptor of the degree of distributed synchrony, the Normalized Euclidian Distance (NED)*

In this type of recurrent networks, provided a balance between excitation and inhibition, the dynamics is usually cyclic with short cycles and total or partial synchrony. We want to quantify the temporal distribution of this synchrony (for details see 4). When, in response to an applied input, the excitatory neurons which participate to the dynamics are active *at each period of the oscillatory cycle*, we consider the activity pattern corresponding to this input to be *a purely spatial code*, since time brings no information. In the opposite case, the activities of the responding excitatory neurons are totally temporally distributed, i.e. the neurons active *at one period of the cycle* are silent during the other periods, in such a way that a specific set of active neurons identifies each period. Such a dynamics represents the optimal use of the temporal dimension. In an intermediate situation, where both spatial and temporal dimensions are combined, the dynamics may exhibit a rich repertoire of spatio-temporal patterns. In our model, the dynamical neuronal behavior involves always the spatial dimension, and more or less the temporal one. We have defined an index (4) which reveals the mean degree of overlapping between subsets of neurons active at different periods of the cyclic global activity, the Normalized Euclidian Distance *NED*. Let us suppose that during this time of observation the dynamics defines T periods of oscillation of the global activity; it is possible to define a distance matrix of size TxT whose general term d_{nm} represents the Euclidian distance between the normalized vectors of neuronal activities at periods n and m respectively, as indicated in Eq. 2.

$$d_{nm} = \sqrt{\sum_{i=1}^{N}\left(\frac{v_{in}}{\|v_{in}\|} - \frac{v_{im}}{\|v_{im}\|}\right)^2} \qquad \text{Eq 2}$$

Then, the Normalized Euclidian Distance represents the mean value of all the terms d_{nm} of the distance matrix, divided by the mean value of the distance matrix taken in the case of the optimal

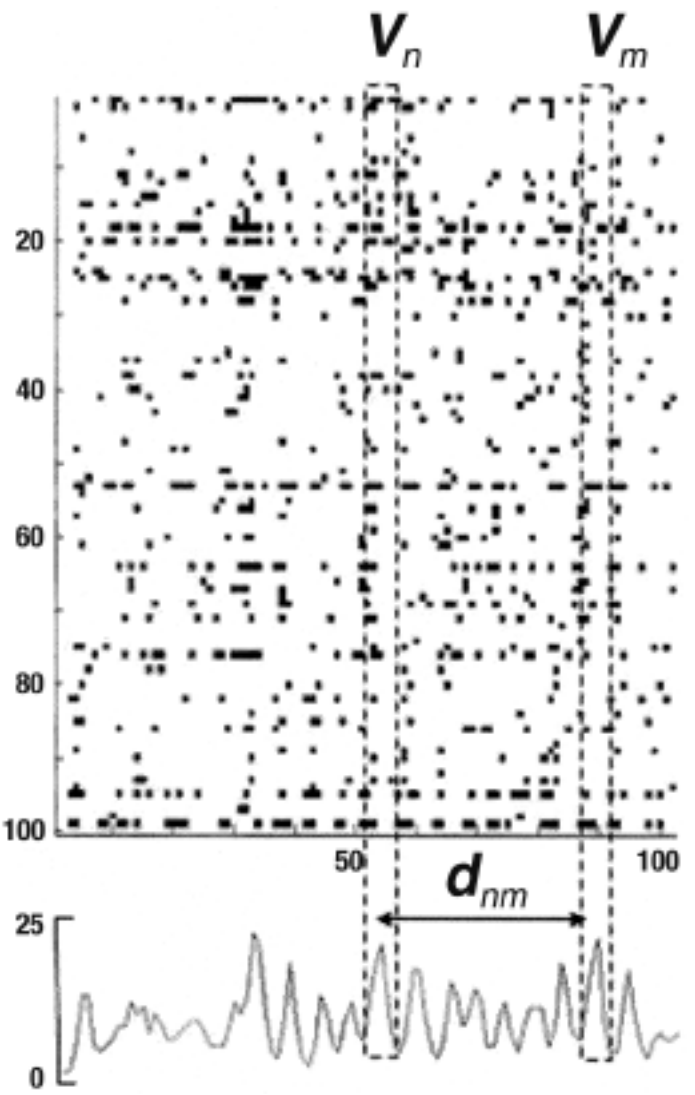

Fig. 1. - *Example of a complex spatio-temporal pattern observed in a recurrent network of MC-P_units connected by a random matrix.*
The upper panel illustrates the activities (black squares) of the 100 excitatory units (PN), the lower panel shows the oscillations of the global activity (time course of number of active neurons).
The distance d_{nm} is computed for every pair of activity vectors V_n, V_m, corresponding respectively to the *n*th and *m*th oscillations.

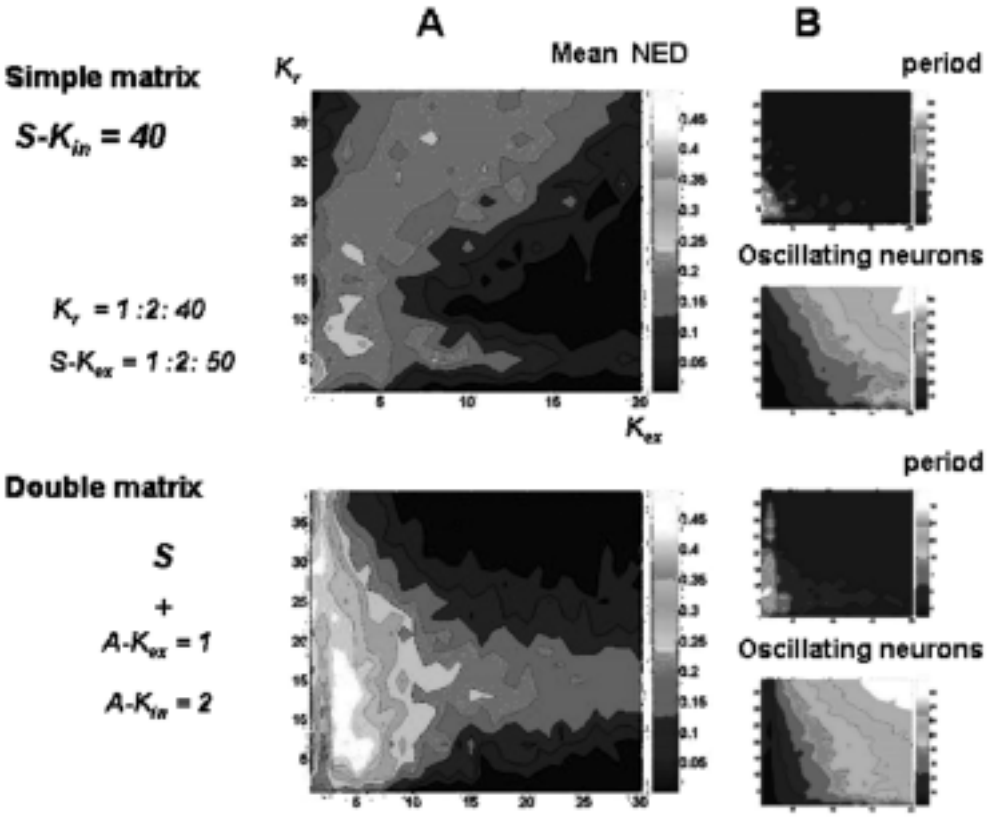

Fig. 2. - *Color maps for the mean value of the Normalized Euclidian Distance (NED) (based on 20 simulations for each point of the bi-dimensional map).*
The values are linearly color-coded to define equidistant contour lines according to the colorbar on the right.
A: Contour maps of *NED* in dependence of two variable network parameters: the connectivity parameters K_{ex} and K_r. There are exceptional *points* with values of *NED>0.4.*
B: Contour maps for the mean dominant period of the oscillatory global activity and for the mean number of oscillating neurons in dependence of the same two variable network parameters: the connectivity K_{ex} and K_r for random matrices.
The upper panels show the maps corresponding to the networks in which the connectivity was defined by matrices of "simple" type (case 1).
The lower panels show the maps corresponding to the networks in which the connectivity was defined by matrices of "double" type (case 2).

use of the temporal dimension. Therefore, in the case of a dynamics where each period of oscillation is defined by a specific set of active neurons, the value of *NED* is 1, while in the case of the pure spatial code, or total synchrony, *NED* is nil.

$$NED = \frac{\sum_{n=1}^{T}\sum_{m=1,n\neq m}^{T} d_{nm}}{\sqrt{2}\cdot T\cdot (T-1)} \qquad \text{Eq 3}$$

Note that for a value of *NED* = 0.5, the corresponding mean overlapping is about 0.7 (see Figure 3 in 4) .

II - Time-continuous Integrate-and-Fire neuron: the Izhikevitch model (IFI)

In the present study, we choose a recently defined Integrate-and-Fire model (5), the Izhikevic Integrate-and-Fire model (IFI). The IFI captures many biological properties of realistic Hodgkin-Huxley type conductance-based models but with a greater simplicity in hardware implementation. In this model, analytically, the potential of each unit is given by a bi-dimensional system of ordinary differential equations of the form:

$$\begin{cases} v' = 0.04v^2 + 5v + 140 - u + I \\ u' = a(bv - u) \end{cases} \quad \text{Eq 4}$$

v represents the membrane potential and a variable *u* is introduced for resetting the membrane potential after the spike reaches its maximal value (set at +30mV) and *a,b* are parameters defining the neuron type. Excitation currents are delivered with the parameter *I*.

An after-spike resetting is defined by the condition, where appear two new parameters *c* and d:

[if *v*=+30 mV]

$$\begin{cases} v \leftarrow c \\ u \leftarrow u + d \end{cases} \quad \text{Eq 5}$$

When implemented in a program, Eq. 4 are discretized using the Euler method; with a time step=1 there is an iteration of Eq. 6:

$$\begin{cases} v_i(t+1) = (0.04v_i(t) + 6) \cdot v_i(t) + 140 - u_i(t) + I_i(t) \\ u_i(t+1) = a_i b_i v_i(t) + (1 - a_i) u_i(t) \end{cases} \quad \text{Eq 6}$$

where the membrane potential $v_i(t)$ and the recovery variable $u_i(t)$ are the variables for the *i*th neurone at time *t*. With the following values for the parameters: *a*=0.02, *b*=0.2, *c*=-65, *d*=2, this model exhibits a simple spiking behavior in response to a steady input current with a linear frequency-intensity relationship like in Hodgkin-Huxley neuron models. Note that, even if such formal neurons, IFI, are necessarily described on the basis of discrete time for computational purposes, the time scale represented here by the integration time step is far smaller than the update time considered in the MC-P model. Indeed, the update time of the MC-P neurons must be larger than the typical refractory period of a neuron, which is one to two order of magnitude greater than an appropriate integration time step which allows an accurate computation of the time course of an action potential. This is why the IFI is considered as a "continuous time" neuron model when compared with the MC-P one. All the simulations based on both types of neuronal models have been performed with MATLAB.

RESULTS

I - Exploring the connectivity parameters with time-discrete MC-P neurons

As there are no biological data for designing a specific connection matrix, we start by examining the dynamics produced by randomly connected networks (case 1: **simple**

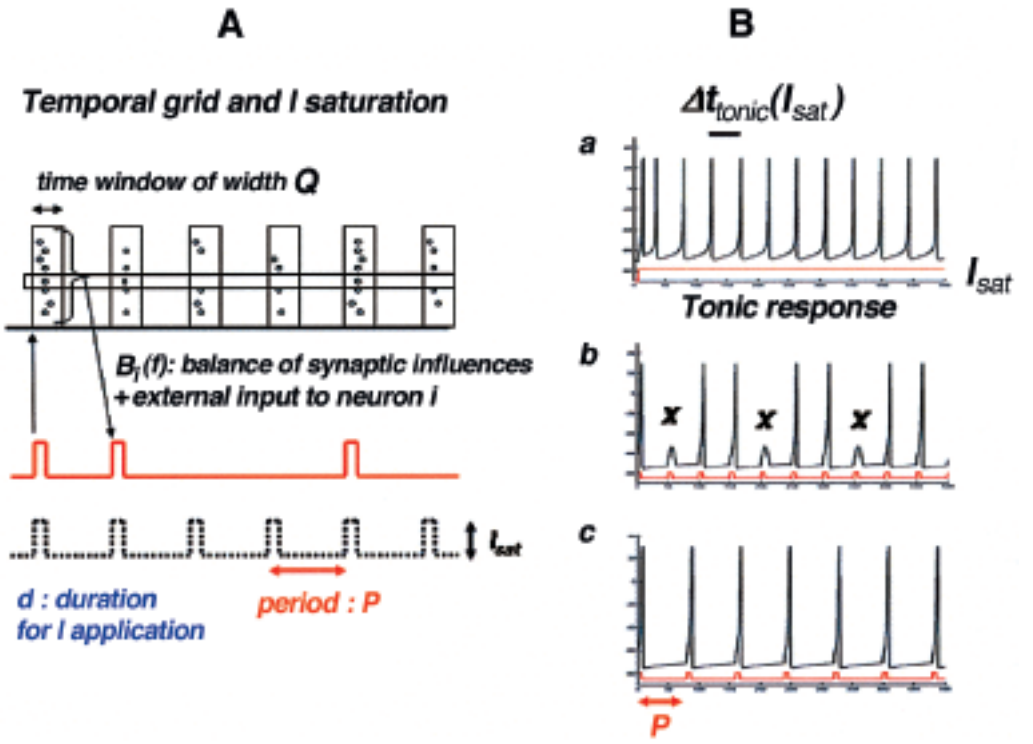

Fig. 3. - *Organization of the temporal grid for a network of IFI neurons.*
A: Definition of parameters Q, P, d and I_{sat} used in the square pulse function $f(t)$ of **Eq7** (dashed line) and $I_i(t)$ of **Eq9** (solid line).
B: Setting P: its value is greater than 1) the interval $\Delta t_{tonic}(I_{sat})$ between two spikes of a tonic response (a) and 2) greater than the necessary time for resetting the membrane potential after a spike induced by a pulse of amplitude I_{sat}, and duration d. In b) the last condition is not satisfied, as some applications of I_{sat} do not drive a spike (missing spikes indicated by X), in c) this condition is satisfied. Setting Q: all spikes must be included in the "observation window".

matrix). In our model networks, with the type of connection matrices defined above, the balance of excitation and inhibition produces different patterns of activity characterized by periodic oscillations corresponding to the fact that the initial group of neurons activated by the input, are inhibited by the network activity, then excited again with a possible recruitment of other neurons, etc… It was recently suggested that some rare strong connections could play a major role in the dynamics of many brain networks (12), such effects were tested by adding to the first random matrix a second connection matrix with very sparse but stronger synaptic weights (case 2: **double matrix**).

In both cases, the standard dynamical behavior of the network is oscillatory, with a period that is very robust with respect to modifications of the synaptic matrix and of the input. In very seldom cases, the dynamics exhibits fixed points. We performed simulations with the following parameters for the input: $K_r = 10$, $W_r = 4$, and for simple synaptic matrix: $K_{ex} = 4$, $W_{ex} = 1$, $K_{in} = 40$, $W_{in} = 5$. *NED* has been computed for

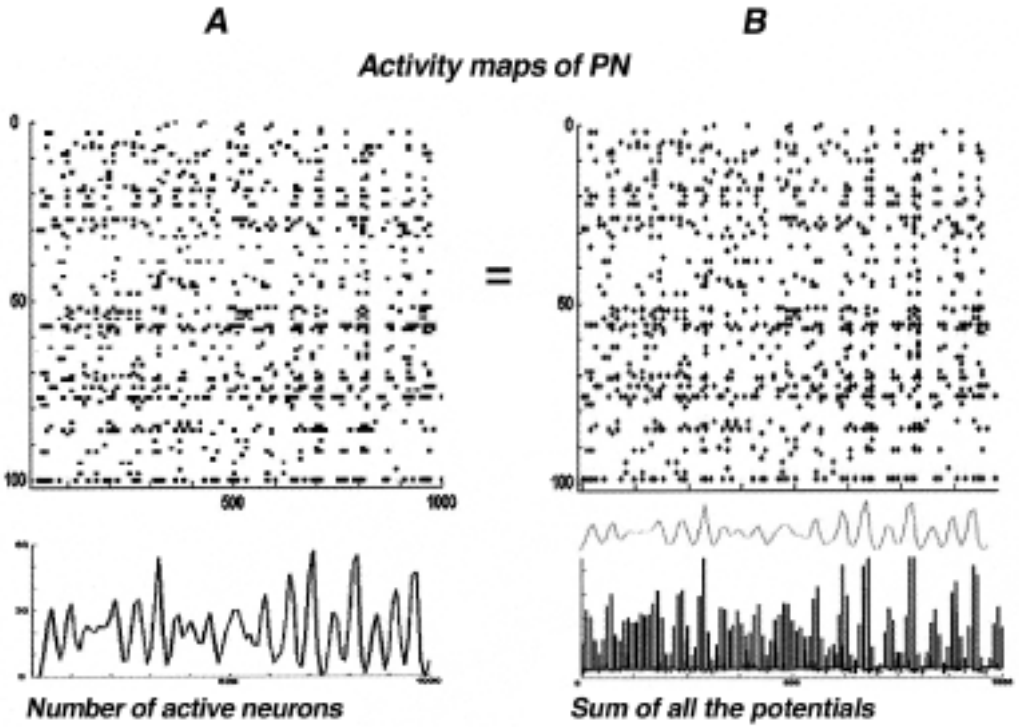

Fig. 4. – *A: Upper panel: Map of the spatio-temporal pattern produced by a recurrent network of MC-P units connected by a double matrix.*
It illustrates the activities (black squares) of the 100 excitatory units (PN). The lower panel shows the time course of the number of active neurons revealing oscillations, base of "the distributed synchrony".
B: Upper panel: Raster plot produced by a recurrent network of IFI neurons connected with the same double matrix, the same delays and receiving the same input as in A. It illustrates the activities (black diamonds) of the 100 excitatory units (PN) which are identical to those of the spatio-temporal map in A. The lower panel illustrates the time course of the sum of membrane potentials. This time course is similar to that of the number of active neurons (red line) shown in A.

each of 5000 random trials in both cases, i.e. for the simple matrix, and the double one, where the additional matrix is characterized by K_{ex} =1, W_{ex} =20, K_{in} =2, W_{in} =10. The effects of adding few, but strong, synaptic weights is illustrated in Fig. 2 showing the value distribution for *NED* in the two cases. With the double matrix, *NED* distribution is clearly shifted towards higher values, around 0.5.

The timing of neuronal spikes in oscillatory networks with partial or total synchrony is under the combined influence of external inputs and internal connections. Thus, we ran batches of simulations in which input connectivity K_r was incremented from 1 to 80 while increasing K_{ex} from 1 to 100 for a fixed value of K_r = 40; we repeated 20 similar batches of simulations for each set of values (K_{ex}, K_r): for each set of these two parameters, we computed the mean value of *NED* from the corresponding 20 simulations. Again, the connectivity patterns corresponding to both cases of simple and double matrices are illustrated in Figure 2. The color-coded

maps, show the bi-dimensional evolutions of *NED* values versus K_{ex} (x axis) and K_r (y axis). The maps focus on a region of interest for the dynamical behavior, i.e., the region where *NED* varies significantly, while there are oscillations for a significant number of excitatory neurons in the network. This region corresponds to values of K_{ex} and K_r respectively in the range of 1-30 and 1-40. Again, the effects of adding some few but strong synaptic weights in the case of the double matrix are clear: with the simple matrix, there are very few *NED* values reaching or exceeding 0.5, in contrast with the double matrix, for which there is a large domain of *NED* values around 0.5. The higher values of *NED* are observed when K_{ex} is in the range 4-10 and K_r in the range 5-15.

These results indicate that it is possible to define connection matrices which lead to spatio-temporal patterns associated to specific clusters of oscillatory neurons at each period of the global cyclic activity. In the case of the double matrix, both periodic dynamical behavior and high values of *NED* are robust against random realizations of this matrix and of the input vector. These possible rich spatio-temporal patterns are similar to those characterized by a "Distributed Synchrony" (8).

II-Comparable dynamics in an IFI network

We now address the question of dynamics in a network of "continuous time" neurons connected by the same synaptic matrix as in the discrete time MC-P network.

In our IFI network model, inhibitory and excitatory neurons have the same characteristics in terms of time constants and threshold. When such neurons are connected to build a network, we consider the mutual influence of the neurons through the value of $I_i(t)$ for each neuron in Eq. 6. Indeed, I_i represents all the influences each neuron i receives: i.e., I_i is a function of the balance between external and internal (from the network) inputs, summing both excitatory and inhibitory effects. At each time step t of the simulation, an appropriate value of $I_i(t)$ has to be defined. Then, the membrane potential of neuron i is computed, and, if at time t, this potential reaches the value of $v_i(t)$=30 mV, the state of neuron i takes the value $n_i(t)$=1, and zero otherwise. It is theoretically possible to update $I_i(t)$ at each time step, according to the states of the presynaptic neurons at (t-1) and the weights of their synapses upon neuron I, however, this computation rule is totally unrealistic since it implies no transmission delays! Therefore, it is necessary to introduce a temporal grid taking into account such delays. Moreover, as we aim to compare the dynamics of the IFI network with the dynamics of the MC-P one, we have to define a temporal grid able to insure the following rule, i.e. every time the balance $B_i(t)$ of all the inputs to a neuron is positive at time t, a short time later, at t', neuron i emits a spike and its state is $n_i(t')$=1, while a negative balance corresponds to the silence of neuron i. This temporal grid is a periodic square pulse function $f(t)$ given in Eq. 7, where P, the period and d the duration of the pulse are the two adjustable parameters. H is the previously defined Heaviside function. This function is the same for all neurons.

$$\begin{cases} f(t) = H(d - r) \\ t = k \cdot P + r \end{cases} \qquad \text{EN} \qquad \text{Eq 7}$$

The balance $B_i(t)$ for neuron i at time t is given by Eq. 8, with a new parameter Q, which represents the width of the time window where the action potentials emitted by presynaptic neurons j are considered.

$$B_i(t) = \sum_{j=1}^{2N} w_{ij} \cdot H\left(\sum_{t'=(k-\tau_{ij})\cdot P}^{(k-\tau_{ij})\cdot P+Q} n_j(t') \right) + R_i - \frac{1}{2} \qquad \text{Eq 8}$$

Finally, the value of $I_i(t)$ is the function defined in Eq 9, based on the temporal grid $f(t)$, which, when non nil, takes the value I_{sat} if $B_i(t)$ is positive and if $f(t)$ equals 1.

$$I_i(t) = I_{sat} \cdot H\left(B_i(t)\right) \cdot f(t) \qquad \text{Eq 9}$$

The parameters P, d and I_{sat} are inter-dependent: once I_{sat} is set, the duration d and the period P of application of I_{sat} have to be chosen from simulations performed on one IFI neuron model, *in order to get a spike in response to every pulse of amplitude I_{sat} and duration d*. Then, the value of Q is chosen greater than the maximal delay of the spiking response to such pulses, in order to include in the "observation window" *all the spikes*.

With this temporal grid defining the update rules, we introduced the network parameters defined for MC-P units in the network of IFI neurons, i.e. the same connection matrix, the same delay matrix and the same input vector. In Fig. 4, upper panels of A and B show activity maps obtained for all PN respectively in model MC-P and IFI models: the dynamics of both network types are *identical*. In addition, the sum of active neurons (Fig. 4A lower panel) exhibits the same time course as the sum of all potentials recorded in the IFI network (Fig. 4B lower panel), thus both of them could be considered as a valid representation of the LFP.

The plots of Fig. 5 show the activities of 4 selected PN amongst the one hundred in the IFI network. They exhibit very different patterns: neuron number 100 is very active while neuron 62 shows few spikes. Note that it is quite difficult to guess a temporal structure from the single recordings of neurons 100 or 85, for instance, while a temporal correlation is apparent when comparing the activities of neurons 71 and 62, where we see that some activities are time-locked. Thus the recording of single neurons is far from being representative of neuronal assemblies!

DISCUSSION

Modeling recurrent networks of excitatory and inhibitory neurons with simple MC-P units, our simulations indicate that connectivity parameters may lead the to the *co-emergence of oscillations and distributed synchrony*, both generating spatio-temporal patterns which are good candidates to represent the formatted codes in the AL of the olfactory system. In order to determine sets of network parameters leading to such a

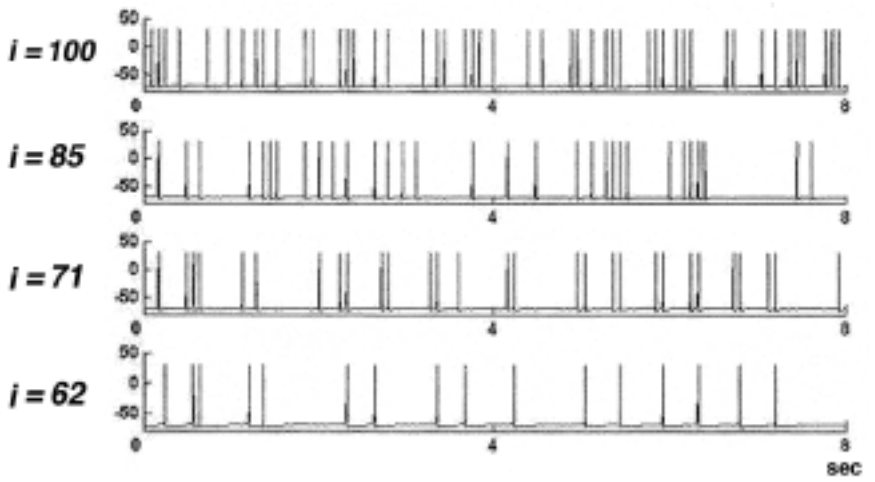

Fig. 5. – *Membrane potentia1s of a sample of 4 IFI neurons selected in the raster plot show in Fig. 4B.*

co-emergence, we have used a descriptor of the degree of distributed synchrony, the *NED*. This index allowed to perform automatic quantification of the use of the temporal dimension in numerous spatio-temporal patterns generated by simulation. With the MC-P neurons, we avoid some computational limitations in modeling neuronal networks: for instance, the huge parameter space linked to conductance-based neuron models requires lots of memory to realize and record the simulation data and much time is needed for processing dynamic updates. Furthermore MC-P networks present the advantage of being analytically tractable for processing information about synaptic matrix and input (4). Our results show that it is possible to capture some features of the insect olfactory system dynamics at the AL stage by using the simplest MC-P model. Concerning the coding possibilities, it is the combination of the *spatial and temporal dimensions* that leads to the richest repertoire of spatio-temporal pattern, with a consequent potential high labeling and classification power with respect to the inputs. However, the "coding capacities", i.e. the discrimination and/or grouping power, need further analyses, in terms of projections from the space of inputs to the space of "outputs", which can be considered at the level of the excitatory neurons studied here, and representing PN in the AL, and, mainly, at the level of the neurons of the next step in the olfactory pathway, i.e., the Kenyon Cells at the level of the mushroom bodies, the last stage of the olfactory pathway (10).

We first explored the dynamics of networks with a random sparse connectivity. Then we introduced some complexity by distributing very sparse stronger weights amongst both PN and LN, and this situation leads more often to dynamics with spatio-temporal patterns of interest (i.e. with a higher *NED*). It was recently suggested that connectivity in many networks could present some non-random features and viewed as "a skeleleton of strong connections in a sea of weaker ones" (12).

Synchronization in the presence of random connectivity has been studied extensively in models using many versions of Integrate and Fire neurons (3, 13). In such studies, the observed dynamics results from a combination of both temporal characteristics of the neurons and the network connectivity, including sometimes synaptic temporal properties. Here, we show the fact that the *connectivity alone*, *without considering any neuronal or synaptic dynamical property*, is able to generate distributed synchrony in the neuronal dynamics. Then, introducing the same connectivity in our IFI network, we can get the same spatio-temporal patterns: the dynamics is clearly driven by the network connectivity. This result should be easily generalized for networks of more realistic conductance-based neurons, since we demonstrated that a small network of Hodgkin-Huxley neurons, with time dependant synapses, may exhibit the same spatio-temporal codes as the ones provided by the equivalent network of MC-P neurons (4).

In both models, each realization of simple or double matrix creates some "modules" embedded in the connectivity structure. Some of them should play major roles in the complexity of the dynamics exhibited by random networks. For instance, the frequency of sub-structures or *loops of local connections* characterized by specific lengths, the distribution of unidirectional, and bidirectional connections may be interesting candidates. This is a new approach to further study dynamics in information-processing networks.

SUMMARY

Both chaotic and periodic activities are observed in networks of the central nervous systems. We choose the locust olfactory system as a good case study to analyze the relationships between networks' structure and the types of dynamics involved in coding mechanisms. In our modeling approach, we first build a fully connected recurrent network of synchronously updated McCulloch and Pitts neurons (MC-P type). In order to measure the use of the temporal dimension in the complex spatio-temporal patterns produced by the networks, we have defined an index the Normalized Euclidian Distance *NED*. We find that for appropriate parameters of input and connectivity, when adding some strong connections to the initial random synaptic matrices, it was easy to get *the emergence of both robust oscillations and distributed synchrony in the spatio-temporal patterns*. Then, in order to validate the MC-P model as a tool for analysis for network properties, we examine the dynamic behavior of networks of continuous time model neuron (Izhikevitch Integrate and Fire model –IFI-), *implementing the same network characteristics.* In both models, similarly to biological PN, the activity of excitatory neurons are phase-locked to different cycles of oscillations which remind the ones of the local field potential (LFP), and nevertheless exhibit dynamic behavior complex enough to be the basis of spatio-temporal codes.

REFERENCES

1. BAZHENOV, M., STOPFER, M., RABINOVICH, M., HUERTA, R. ABARBANEL, HD., SEJNOWSKI, TJ., LAURENT, G. Model of transient oscillatory synchronization in the locust antennal lobe. *Neuron*, **30**: 553-567, 2001.
2. BAZHENOV, M., STOPFER, M., RABINOVICH, M., ABARBANEL, HD., SEJNOWSKI, TJ., LAURENT, G. Model of cellular and network mechanisms for odor-evoked temporal patterning in the locust antennal lobe. *Neuron*, 30: 569-581, 2001.
3. BRUNEL, N. Dynamics of sparsely connected networks of excitatory and inhibitory spiking neurons. *J. Comput. Neurosci*, 8:183-208, 2000.
4. HORCHOLLE-BOSSAVIT, G., QUENET, B., FOUCART, O. Oscillation and coding in a formal neural network considered as a guide for plausible simulations of the insect olfactory system. *Biosystems*. 2006; *in press.*
5. IZHIKEVICH, E.M. Simple model of spiking neurons. *IEEE Transactions on Neural Networks*, 14:1569-1572, 2003.
6. LAURENT, G. Dynamical representation of odors by oscillating and evolving neural assemblies. *Trends Neurosci.*, **19**: 489-496, 1996.
7. LAURENT, G. Olfactory network dynamics and the coding of the multidimensional signals. *Nature*, 3, 883-895, 2002.
8. LEVY, N., HORN, D., MEILIJSON, I., RUPPIN, E. Distributed Synchrony in a Cell Assembly of Spiking Neurons. *Neural Networks*, **14**: 815-824, 2001.
9. MACLEOD, K., LAURENT, G. Distinct mechanisms for synchronization and temporal patterning of odor-encoding neural assemblies. *Science* **274**: 976-979, 1996.
10. MAZOR, O., LAURENT, G. Transient dynamics versus fixed points in odor representations by locust antennal lobe projection neurons. *Neuron*, **48**: 661-673, 2005.
11. NOWOTNY, T., HUERTA, R. Explaining synchrony in feed-forward networks: Are McCulloch-Pitts neurons good enough? *Biol. Cybern*, **89**: 237-241, 2003.
12. SONG, S. SJOSTROM, P.J., REIGL, M., NELSON, S., CHKLOSVSKII, D.B. Highly nonrandom features of synaptic connectivity in local cortical circuits. *PLoS Biol.*, 3:e68, 2005.
13. VOGELS, T.P., RAJAN, K., ABBOTT, L.F. Neural network dynamics. *Annu.Rev. Neurosci.*, **28**: 357-376, 2005.
14. WEHR, M., LAURENT, G. Odour encoding by temporal sequences of firing in oscillating neural assemblies. *Nature*, **384**: 162-166, 1996.